

# HEAR: Human Action Recognition via Neural Networks on Homomorphically Encrypted Data

Miran Kim<sup>1,2</sup>, Xiaoqian Jiang<sup>3</sup>, Kristin Lauter<sup>4</sup>, Elkhan Ismayilzada<sup>1</sup>, Shayan Shams<sup>3</sup>

<sup>1</sup> Department of Computer Science and Engineering, Ulsan National Institute of Science and Technology

<sup>2</sup> Graduate School of Artificial Intelligence, Ulsan National Institute of Science and Technology

<sup>3</sup> School of Biomedical Informatics, University of Texas, Health Science Center at Houston

<sup>4</sup> Facebook AI Research

**Abstract**—Remote monitoring to support “aging in place” is an active area of research. Advanced computer vision technology based on deep learning can provide near real-time home monitoring to detect falling and symptoms related to seizure, and stroke. Affordable webcams, together with cloud computing services (to run machine learning algorithms), can potentially bring significant social and health benefits. However, it has not been deployed in practice because of privacy and security concerns. People may feel uncomfortable sending their videos of daily activities (with potentially sensitive private information) to a computing service provider (e.g., on a commercial cloud). In this paper, we propose a novel strategy to resolve this dilemma by applying fully homomorphic encryption (FHE) to an alternative representation of human actions (i.e., skeleton joints), which guarantees information confidentiality while retaining high-performance action detection at a low cost. We design an FHE-friendly neural network for action recognition and present a secure neural network evaluation strategy to achieve near real-time action detection. Our framework for private inference achieves an 87.99% recognition accuracy (86.21% sensitivity and 99.14% specificity in detecting falls) with a latency of 3.1 seconds on real-world datasets. Our evaluation shows that our elaborated and fine-tuned method reduces the inference latency by 23.81%~74.67% over a straightforward implementation.

**Index Terms**—Homomorphic encryption, action recognition, convolutional neural networks

## I. INTRODUCTION

Human action recognition has emerged as an important area of research in computer vision due to its potential applications in video surveillance, telemedicine, human-computer interaction, ambient assisted living, robotics, etc. In particular, the application to telemedicine is becoming more critical as changes in demographics, such as declining fertility rate and increasing longevity of older adults, have made the ability to provide remote healthcare more important than ever before [1], [4], [40]. While machine learning can provide real-time face detection and activity recognition (e.g., detecting behavioral pattern changes, emotion, falling, and seizure), the privacy concern has become a critical hurdle in providing virtual (remote) care to patients, especially in the cloud-based computing environment. Cloud-based services are becoming the mainstream in online marketplaces of digital services due to cost-effectiveness and robustness. On the other hand, edge devices have limited capacity to support miscellaneous and

ever-growing types of digital services, which makes data and computation outsourcing to the cloud a natural choice. But individual clients do not want sensitive personal data to share with service providers.

In this paper, we propose a secure service paradigm to reconcile the critical challenge by integrating machine learning and *Fully Homomorphic Encryption* (FHE). FHE enables us to perform high-throughput arithmetic operations on encrypted data without decryption. The synergistic combination of technologies enables the cloud to process encrypted data to allow real-time monitoring of the elderly with mitigated privacy concerns.

In general, human action can be recognized from multiple modalities such as RGB images or video, depth, and body skeletons. Among these modalities, dynamic human skeletons, representing 2D or 3D joint coordinates, have attracted more attention since they are robust against dynamic circumstances and are highly efficient in computation and storage [19], [42], [44]. Compared to the conventional handcrafted-based method [25], [46], [47], the deep learning based modeling approach can automatically learn the action features using recurrent neural networks (RNN) [36], [50], convolutional neural networks (CNN) [29], [32], and graph convolutional networks (GCN) [43], [48]. In this work, we adopt the CNN-based approach for skeleton-based action recognition. The skeleton joints are easily captured by the depth sensors or the pose estimation algorithms [11], [23], [45]. Fig. 1 illustrates a pipeline of cloud-based action recognition framework, where FHE serves as a bridge to turn intrusive video monitoring into trustworthy services. The detected joint keypoints in consecutive frames are encrypted and sent to a cloud service provider. After private action recognition, the encrypted results are transmitted to a trusted party (e.g., a nursing home) who decrypts them and decides if immediate intervention is necessary (e.g., fall or seizure is detected to call the responders).

Although significant progress on FHE has been made towards improving efficiency, there remains a sizable gap between this technology and the adoption to practical applications. A ciphertext in HE cryptosystem has an inherent error for security and multiplication operations bring about an in-

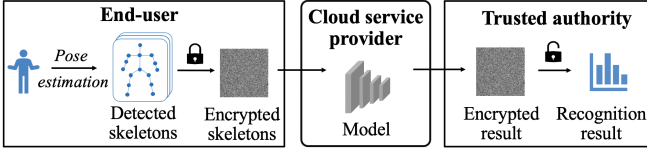


Fig. 1: A pipeline of cloud-based action recognition framework.

creased noise level. So we should select encryption parameters to ensure security and correctness of decryption. Moreover, as homomorphic operations result in different computational costs (e.g., multiplication is a more costly operation than others), it is imperative to balance multiplicative circuit depth and computation cost. In particular, the Cheon-Kim-Kim-Song (CKKS) [13] scheme is considered to be one of the best-performing FHE cryptosystems in terms of amortized time per plaintext and expansion rate. Despite its versatility, several usability issues prevent its widespread use in practice.

#### A. Our contributions

We present an FHE-friendly CNN for skeleton-based action recognition, which is designed specially to be computed by a small-depth circuit along with low-degree activation functions (with parameters adjusted during the training process). Based on the proposed neural networks, we design a novel framework, namely Homomorphically Encrypted Action Recognition (HEAR), which is a scalable and low-latency system to perform secure neural network inference for the action recognition task.

We first present a simple yet effective tensor data encryption method to extensively use the plaintext space within an encryption parameter limit. Each 2D channel of a 3D input tensor is converted to a 1D vector in row-major format and we stack copies of their concatenation as many as possible, resulting in a fully-packed ciphertext. We then introduce an efficient evaluation strategy to leverage parallel computation on packed ciphertexts in a single instruction multiple data (SIMD) manner while maintaining our unique small-footprint data representation throughout the whole evaluation process. We exploit the ciphertext packing technique to represent multiple nodes of layers as the same ciphertext. We express convolution operations as FHE-friendly operations on packed ciphertexts (e.g., SIMD addition/multiplication, scalar multiplication, and slot rotation).

Our main observation is to investigate the sparsity of ciphertexts obtained by downsampling (i.e., pooling layer). The integration of the pooling and convolution operations has not been studied in depth. Juvekar et al. [28] presented a fast homomorphic convolution operation, but the result of a pooling layer is freshly encrypted as a fully-packed ciphertext that is the input to the subsequent convolutional layer, which is not our case. In the secure outsourcing framework, we get a ciphertext with non-valued values by accumulating the adjacent entries for downsampling. We present a fast HEAR framework

(Fast-HEAR) that enables us to put together such sparsely-packed ciphertexts with valid values and perform simultaneous homomorphic convolution operations over packed ciphertexts. The partial convolution results are contained in the resulting ciphertexts, and these can be easily summed together across plaintext slots. We also come up with optimizations tailored for CKKS-based secure inference on the proposed neural networks. We observe that the trained model parameters can be computed with low-level ciphertexts. So, we present the level-aware encoding method to represent the weight parameters as a plaintext polynomial with small-sized coefficients with support for such ciphertexts. As a result, Fast-HEAR brings notable performance improvement with drastic size reduction in trained models.

We empirically demonstrate the effectiveness of our private inference system over three benchmark datasets: the J-HMDB dataset [27], the UR Fall Detection dataset [33], and the Multiple cameras fall dataset [6]. HEAR enables a single prediction in *12.2 seconds* on a 2D neural network model for action recognition tasks while achieving an 87.99% recognition accuracy and 86.21% sensitivity in detecting falls. Our elaborated and fine-tuned solution of Fast-HEAR can evaluate the same neural network in *3.1 seconds* using only a few Gigabytes of RAM. The intensive use of space and SIMD computation in Fast-HEAR reduces the trained model encoding time by 51.99%~86.41% and the inference latency by 23.81%~74.67% over HEAR. Moreover, it results in a significant reduction in memory usage for encoded model parameters, using 86% less space than HEAR. To the best of our knowledge, this is the first work to homomorphically evaluate the neural networks for skeleton-based action recognition tasks on large-scale datasets.

## II. BACKGROUND AND RELATED WORKS

### A. The CKKS scheme

Fully homomorphic encryption is a cryptosystem that allows for operations on encrypted inputs without decryption. Among the efficient FHE schemes, the CKKS scheme [13] is a unique solution that supports approximate computation on encrypted data. This scheme provides a trade-off between efficiency and precision, but it has shown remarkable performance advantages in real-world applications that do not require absolute precision [30], [31]. The recent deep learning research has demonstrated low precision multiplications as an effective way to accelerate training and inference [34]. This low-precision optimization strategy matches a key feature of the CKKS scheme, which uses a built-in *rescaling* operation on encrypted data as if rounding off significant digits in plain fixed-point computation.

Throughout the paper, we assume that  $N$  is a power-of-two integer and  $R = \mathbb{Z}[X]/(X^N + 1)$ . We write  $R_q = R/(q \cdot R)$  for the residue ring of  $R$  modulo an integer  $q$ . The CKKS scheme [13] is a leveled HE scheme with support for approximate fixed-point arithmetic. We assume  $q = \prod_{i=0}^L p_i$  for some integers  $p_i$  to have a chain of ciphertext moduli  $q_0 < q_1 < \dots < q_L$  for  $q_\ell = \prod_{i=0}^\ell p_i$ . For homomorphic

operations between ciphertexts at different levels, it requires to transform a high-level ciphertext to have the same level as the other. The following is a simple description of CKKS based on the ring learning with errors (RLWE) problem.

- **Setup( $1^\lambda$ )**: For a given security parameter  $\lambda$ , set the RLWE dimension  $N$ , ciphertext modulus  $q$ , key distribution  $\chi$  and error distribution  $\psi$  over  $R$ . Generate a random vector  $a \leftarrow U(R_q)$ . Return the public parameter  $pp = (n, q, \chi, \psi, a)$ .
- **KeyGen( $pp$ )**: Sample the secret key  $s \leftarrow \chi$ . Sample an error vector  $e \leftarrow \psi^d$  and set  $b = -s \cdot a + e \pmod{q}$ . Set the public key  $pk = (b, a)$ .
- **Enc( $m; pk$ )**: Let  $m \in R$  be an input plaintext. Return the ciphertext  $ct = (c_0, c_1) \in R_q^2$  where  $c_0 = v \cdot b + m + e_0 \pmod{q}$  and  $c_1 = v \cdot a + e_1 \pmod{q}$ .
- **Dec( $ct; s$ )**: Let  $ct = (c_0, c_1) \in R_{q_\ell}^2$  be a ciphertext at level  $\ell$ . Set  $sk = (1, s)$  and return  $\langle ct, sk \rangle \pmod{q_\ell}$ .
- **Add( $ct_1, ct_2$ )**: Given two ciphertexts  $ct_i \in R_{q_\ell}^2$  at level  $\ell$ , return the ciphertext  $ct' = ct_1 + ct_2 \pmod{q_\ell}$ .
- **Mult( $ct_1, ct_2$ )**: Given two ciphertexts  $ct_i \in R_{q_\ell}^2$  at level  $\ell$ , compute  $ct = ct_1 \otimes ct_2 \pmod{q_\ell}$  and return the ciphertext  $ct' \leftarrow \text{Relin}(ct) \in R_{q_\ell}^2$ .
- **Rescale( $ct$ )**: Given a ciphertext  $ct = (c_0, c_1) \in R_{q_\ell}^2$  at level  $\ell$ , compute  $c'_i = \lfloor p_\ell^{-1} \cdot c_i \rfloor$  for  $i = 0, 1$ , and return the ciphertext  $ct' = (c'_0, c'_1) \in R_{q_{\ell-1}}^2$ .

The CKKS scheme supports the *ciphertext packing technique* to encrypt vectors of elements and perform parallel homomorphic operations in a SIMD manner. A ciphertext can hold up to  $N/2$  plaintext values:

$$\begin{aligned} \text{Dec}(\text{Enc}(x) + \text{Enc}(y)) &\approx x \oplus y, \\ \text{Dec}(\text{Enc}(x) \cdot \text{Enc}(y)) &\approx x \odot y, \end{aligned}$$

where  $\oplus$  and  $\odot$  denote the element-wise addition and multiplication, respectively. Furthermore, it allows one to perform the rotation algorithm, denoted by  $\rho^\ell(ct)$ , which transforms an encryption  $ct$  of  $v = (v_0, \dots, v_{N/2-1})$  into an encryption of  $\rho^\ell(v) := (v_\ell, \dots, v_{N/2-1}, v_0, \dots, v_{\ell-1})$ . We note that  $\ell$  can be either positive or negative, and a rotation by  $(-\ell)$  is the same as a rotation by  $(N/2 - \ell)$ .

### B. Related works

CryptoNets [20] was the first protocol to demonstrate private neural network inference, showing inference on the MNIST dataset by using a square activation function in the neural network. Their protocol represents each node in the network as distinct ciphertexts while making predictions on thousands of inputs at a time. The follow-up works [8], [15] significantly improved the throughput. However, they have high latency even for a single prediction, so it is not a viable solution for large-scale neural network models.

In other recent works, the TFHE scheme [14] was used for secure neural network inference on Boolean circuits [9]. But it is relatively slow for integer arithmetic, which limits

the practical applicability in large neural networks for time-sensitive tasks. In the SHE system [37], the ReLU and max-pooling are expressed as Boolean operations and implemented by the TFHE homomorphic Boolean gates. Although SHE achieves state-of-the-art inference accuracy on the CIFAR-10 dataset, it requires thousands of seconds to make inference on an encrypted image.

The most relevant studies are by LoLa [10], CHET [17], and EVA [16], which use the ciphertext packing method to represent multiple values from network nodes as the same ciphertext. In LoLa [10], the convolution layer is expressed as a restricted linear operation by flattening the filters or a series of dot products between a data vector and each row of a weight matrix. As a consequence, it requires a substantial number of rotations for an evaluation of wide neural networks. In an orthogonal direction, CHET [17] and EVA [16] are FHE-based optimizing compilers to make secure predictions easier by simplifying neural networks to homomorphic circuits. Their general-purpose solutions cannot fully take advantage of advanced techniques of FHE, so they may not be optimal for all tasks in terms of both time and space. In contrast to their generalized approach, we present a secure and scalable evaluation strategy targeted for action recognition tasks on considerably wide networks. Our approach is efficient in computation complexity by exploiting the plaintext space and performing homomorphic convolutions in parallel.

There are other approaches for privacy-preserving deep learning prediction based on multi-party computation [7], [39] and their combinations with HE [28], [35]. They provide good latency but assume the tolerance of a high communication overhead, which is not feasible in practice.

## III. METHOD

In this section, we present a low-latency optimized algorithm to evaluate the proposed neural network on encrypted data.

**Threat model.** In our paradigm, model providers train a neural network with plaintext dataset in the clear and provision of its model to a public cloud. Then, the cloud server provides an online prediction service to data owners who uploaded their encrypted data. We assume that the cloud server is semi-honest. Thus, if we ensure the IND-CPA security of an underlying HE scheme, one can ensure the confidentiality of data against such a semi-honest server (i.e. honest but curious)

**Network architecture.** Suppose that we are given 3D arrays with dimension  $T \times J \times 2$  where  $T$  is the number of frames of the skeleton sequence in the video and  $J$  is the number of skeleton joints in each frame. The action recognition network is inspired by the design of [18] to capture spatial-temporal information. The network consists of three convolutional layers with a filter size of 3 (1D-CNN) or  $3 \times 3$  (2D-CNN), a stride of 1, and the same padding. We follow the design rule of ResNet [24] such that if the feature map size is halved, the width (the number of channels) is increased to double. Each convolutional layer is followed by batch normalization (BN).

The downsampling is performed by average-pooling over  $2$  or  $2 \times 2$  window with a stride of  $2$ . The network ends with a global average pooling, a fully-connected layer, and softmax. We remark that the final step of the neural network is to apply the softmax function for probabilistic classification, so it is enough to obtain an index of maximum values of outputs in a prediction phase.

**Notation.** If two matrices  $A_1$  and  $A_2$  have the same number of rows,  $(A_1|A_2)$  denotes a matrix formed by horizontal concatenation. We use a row-major ordering encoding map to transform a matrix in  $\mathbb{R}^{d_1 \times d_2}$  into a vector of dimension  $n = d_1 d_2$ . More specifically, for a vector  $\mathbf{a} = (a_k)_{0 \leq k < n}$ , we define the encoding map  $\text{mat} : \mathbb{R}^n \rightarrow \mathbb{R}^{d_1 \times d_2}$  by

$$\text{mat} : \mathbf{a} \mapsto \mathbf{A} = (a_{d_2 \cdot i + j})_{0 \leq i < d_1, 0 \leq j < d_2}, \quad (1)$$

i.e.,  $\mathbf{a}$  is the concatenation of row vectors of  $\mathbf{A}$ . Let  $\text{vec}$  denote its inverse mapping. We use  $\text{padZeros}(\mathbf{A}; \mathbf{v}, \text{dir})$  to pad a matrix  $\mathbf{A}$  with zeros in the direction specified by  $\text{dir}$  where  $\mathbf{v}$  is a vector of non-negative integers that specifies both the amount of padding to add and the dimension along which to add it. The direction can be specified as one of the following values: L (left), R (right), U (upper), and B (bottom). We denote by  $\text{PoT}(x)$  the smallest power-of-two integer that is greater than  $x$ .  $\text{rep}(\mathbf{A}; \ell_1, \ell_2)$  returns an array containing  $\ell_1$  and  $\ell_2$  copies of  $\mathbf{A}$  in the row and column dimensions, respectively.

#### A. Data encryption

Since the CKKS scheme supports homomorphic operations only on encrypted vectors, an input tensor needs to be converted into such a plaintext format. Based on the estimated skeleton joints of size  $T \times J \times 2$ , each 2D channel of size  $T \times J$  is first converted to a 1D vector in row-major format. Then it is zero-padded on the right to make the vector size as a powers-of-two. Let  $N_2 = N/2$ , which is the maximal length of plaintext vector from the encryption parameter setting (we refer the reader to Section IV-A for detailed descriptions). We then stack  $N_2/(\text{PoT}(T \cdot J) \cdot 2)$  copies of the input tensor while interlacing the input channels, so that we can fully exploit the plaintext space for homomorphic computation. Afterward, we encrypt it as a fully-packed ciphertext. We remark that if we do not pad with extra zero entries and make multiple copies of the input as many as possible, then the resulting plaintext vector has zeros in the last few entries, resulting in different rotation results in those positions.

Algorithm 1 takes as input  $\mathcal{X} = (X_1, X_2)$  with  $X_i \in \mathbb{R}^{T \times J}$ , and outputs the encryption  $\text{ct}_{\mathcal{X}}$ .

#### B. Homomorphic convolution

We start with a simple convolution of a single input in  $\mathbb{R}^{h \times w}$  with a single channel. As the filter slides through the input, we perform element-wise multiplication and addition at each sliding position. If the input is encrypted as a single ciphertext in row-major format, we can get the convolution results at all the positions at a time. This can be achieved by simply computing  $f_h \cdot f_w$  rotations of the encrypted input and

#### Algorithm 1 Encryption of skeleton data

**Input:**  $\mathcal{X} = (X_1, X_2) \in \mathbb{R}^{T \times J} \times \mathbb{R}^{T \times J}$

**Output:**  $\text{ct}_{\mathcal{X}}$ , a fully-packed ciphertext

```

1:  $n \leftarrow T \cdot J$ 
2: for  $1 \leq i \leq 2$  do
3:    $\mathbf{m}_i \leftarrow \text{padZeros}(\text{vec}(X_i); (\text{PoT}(n) - n), \text{R})$ 
4: end for
5:  $\mathbf{m} \leftarrow (\mathbf{m}_1 | \mathbf{m}_2) \in \mathbb{R}^{2 \cdot \text{PoT}(n)}$ 
6:  $\bar{\mathbf{m}} \leftarrow \text{rep}(\mathbf{m}; N_2 / (2 \cdot \text{PoT}(n))) \in \mathbb{R}^{N_2}$ 
7:  $\text{ct}_{\mathcal{X}} \leftarrow \text{Enc}(\bar{\mathbf{m}})$ 
8: return  $\text{ct}_{\mathcal{X}}$ 
```

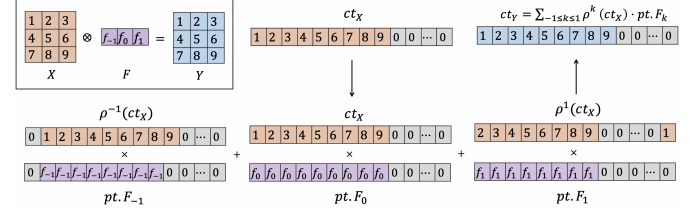


Fig. 2: An illustration of homomorphic evaluation of simple 1D convolution with a kernel size of 3.

multiplying each ciphertext by a plaintext polynomial with the weights of the filter. The simple convolution can be computed by evaluating

$$\text{H-Conv}(\text{ct}) = \sum_{|k| \leq f} \text{MultPlain}(\rho^{r_k}(\text{ct}), \text{pt.F}_k), \quad (2)$$

where  $\text{ct}$  denotes an input ciphertext,  $\text{pt.F}_k$ 's are the plaintext polynomials which have the weights of the filters in appropriate locations,  $r_k$ 's denote rotation amounts for the simple convolution,  $f$  is defined as  $\frac{1}{2}(f_h \cdot f_w - 1)$ , and  $\text{MultPlain}(\text{ct}, \text{pt})$  denotes a multiplication of a plaintext  $\text{pt}$  to a ciphertext  $\text{ct}$ . As illustrated in Figures 2 and 3, we see that  $r_k = \{0, \pm 1\}$  or  $r_k = \{0, \pm 1, \pm 2, \pm 3, \pm 4\}$  for the simple 1D or 2D convolution, respectively.

The multi-channel convolution is represented as  $c$  filter banks  $\{F_j \in \mathbb{R}^{f_h \times f_w \times c}\}_{1 \leq j \leq c}$  on an input tensor  $\mathcal{X} = \{X_i \in \mathbb{R}^{h \times w}\}_{1 \leq i \leq c}$ . Fig. 4a illustrates the plain multi-channel convolution with  $c$  filter banks on the input tensor  $\mathcal{X}$ . For the sake of brevity, we assume that the input  $\mathcal{X}$  is given as a fully-packed ciphertext. We start with the first filter  $F_1 = \{F_{1i} \in \mathbb{R}^{f_h \times f_w}\}_{1 \leq i \leq c}$ . As shown in Fig. 4b, the homomorphic convolution consists of two steps: (i) *Extra-rotation*: the input ciphertext is rotated by multiples of  $h \cdot w$  (which corresponds to a kernel-wise process) and (ii) *Intra-rotation*: at each rotating position  $i$ , we perform a single-channel convolution on the rotated ciphertext of the input channel  $X_i$  with the kernel  $F_{1i}$  as in Eq. (2). We repeat such a process for all the rotating positions and sum up the results to generate one single output channel. Since we use only the first  $h \cdot w$  entries for the convolution with  $F_1$ , we can pack together  $c$  distinct kernels of the feature maps in plaintext slots and perform  $c$  simple convolutions simultaneously in a SIMD

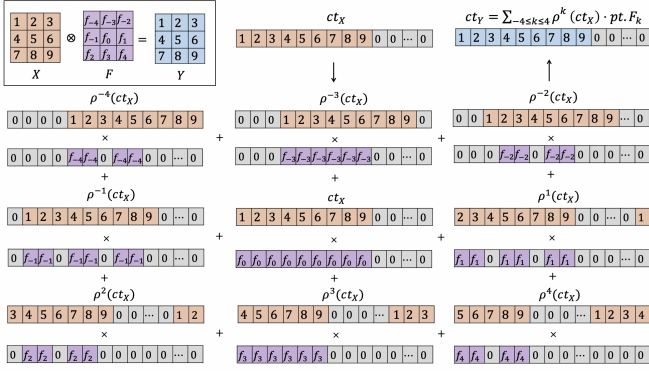


Fig. 3: An illustration of homomorphic evaluation of simple 2D convolution with a kernel size of  $3 \times 3$ .

manner without additional cost, resulting in a ciphertext that represents  $c$  output channels stacked together.

In general, let  $\ell_I$  and  $\ell_O$  denote the numbers of input and output channels to be packed into a single ciphertext, respectively. We denote by  $n_I = \lceil c_I / \ell_I \rceil$  and  $n_O = \lceil c_O / \ell_O \rceil$  the number of input and output ciphertexts, respectively. For  $j = 1, 2, \dots, n_O$ , the results of multi-channel convolution of the  $j$ -th output block can be securely computed by

$$\begin{aligned}
 & \text{H-Conv}_j(\text{ct}_1, \dots, \text{ct}_{n_I}) \\
 &= \sum_{1 \leq i \leq n_I, 0 \leq \ell < \ell_I} \text{H-SConv}(\rho^{h \cdot w \cdot \ell}(\text{ct}_i)) \\
 &= \sum_{1 \leq i \leq n_I, |k| \leq f, 0 \leq \ell < \ell_I} \text{MultPlain}(\rho^{r_k + h \cdot w \cdot \ell}(\text{ct}_i), \text{pt.F}_{i,j,k,\ell}), \quad (3)
 \end{aligned}$$

where  $\text{ct}_i$  denotes a ciphertext which represents the tensor input obtained by extracting from the  $(\ell_I \cdot (i-1))$ -th channel to  $((\ell_I \cdot i) - 1)$ -th channel,  $\text{pt.F}_{i,j,k,\ell}$ 's are the plaintext polynomials which have the weights of the filters in appropriate locations,  $r_k$  indicates a rotation amount for the simple convolution. To be precise, the output ciphertext represents from  $(\ell_O \cdot (j-1))$ -th output channel to  $((\ell_O \cdot j) - 1)$ -th output channel.

### C. Fast homomorphic convolution

We observe that an average pooling layer can be implemented by accumulating the entries across plaintext slots. To be more precise, if we first rotate the ciphertext by one and add it to the input, then we get a ciphertext whose entries contain the sums of two adjacent elements. By repeating this procedure with an appropriate amount of rotation, it yields a ciphertext such that the sum for each patch on the feature map is placed in the leftmost entry of the patch, whereas all slots except these actual result components contain redundant partial sums.

We propose a fast HEAR framework with *merge-and-conquer* method, which extensively uses the components with non-valid values for more SIMD parallelism of the subsequent

computation (i.e., homomorphic convolution right after down-sampling). For a convolutional layer with  $c_O$  feature maps of size  $c_I$ , we achieve this in three steps. We assume that each input ciphertext has valid values of  $c$  input channels for some constant  $c > 0$ . (i) As shown in Fig. 5a, we first multiply the output ciphertexts of the pooling layer by a constant zero-one plaintext vector to annihilate the junk entries marked #. As mentioned above, these non-valid entries are derived from the previous pooling operation. Then we rotate each ciphertext by an appropriate amount and sum up all the resulting ciphertexts, yielding a new ciphertext that contains all the valid entries of inputs. We define the *load factor*  $n_P$  as the number of input ciphertexts to fit into a single ciphertext (e.g.,  $n_P = 4$  in Fig. 5a). Then we need  $n_P$  constant-ciphertext multiplications and  $(n_P - 1)$  rotations. Now each output ciphertext contains  $(c \cdot n_P)$  valid values. (ii) We then proceed the aforementioned ordinary homomorphic convolution with  $c_I / (c \cdot n_P)$  input ciphertexts, in which each ciphertext contains not  $c$  results but  $(c \cdot n_P)$  partial convolution results. (iii) Once this is done, we accumulate these results across plaintext slots by doing precisely the opposite of the first step to get  $c$  actual convolution results. As illustrated in Fig. 5b, the partial results are summed together, yielding a ciphertext of the same form as the original output of the pooling layer. It can be implemented with  $(n_P - 1)$  rotations with the same amounts in the reverse direction. Moreover, we can reduce the number of rotations down to  $\lceil \log_2 n_P \rceil$  rotations by accumulating them with recursive rotate-and-sum operations as illustrated in Fig. 5b.

Consequently, Fast-HEAR incurs an additional cost to incorporating values at distinct ciphertexts (pre-processing) and aggregating values located in different slots (post-processing). However, the computational complexity of the second ordinary convolution step is reduced by a factor of  $n_P$  compared to HEAR, which allows greater efficiency. In Section III-D, we will provide a detailed comparison of HEAR and Fast-HEAR in the context of theoretical complexity. This method has another advantage, in that it substantially reduces the amount of memory required for plaintext polynomials of filters. It reduces the number of plaintexts by a factor of  $n_P$  since the filters are packed more tightly in plaintext polynomials than HEAR.

Algorithm 2 provides a description of homomorphic convolution in Fast-HEAR. We note that in 1D-CNN, we define the rotation amounts  $\mu_i$  and  $\nu_j$  as

$$\begin{aligned}
 \mu_i &= i - 1, \\
 \nu_j &= 2^{j-1},
 \end{aligned}$$

for  $1 \leq i \leq n_P, 1 \leq j \leq \lceil \log_2(n_P) \rceil$ . Here,  $\mu_i$  and  $\nu_j$  are used for the pre-processing and post-processing steps, respectively. In 2D-CNN, we define the rotation amounts as

$$\begin{aligned}
 \mu_{i+k\sqrt{n_P}} &= (i-1) + k \cdot w, \\
 \nu_{j+k' \log_2(\sqrt{n_P})} &= k' \cdot 2^{j-1},
 \end{aligned}$$



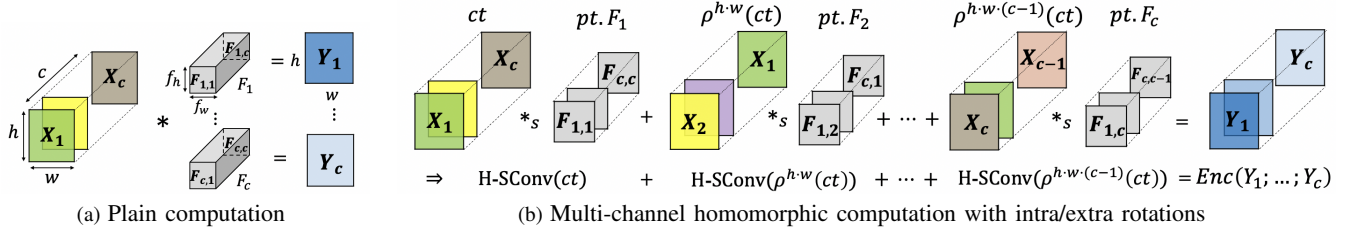


Fig. 4: Plain and homomorphic convolution algorithms of the feature maps  $\{F_j \in \mathbb{R}^{f_h \times f_w \times c}\}_{1 \leq j \leq c}$  on an input  $\mathcal{X} = \{X_i \in \mathbb{R}^{h \times w}\}_{1 \leq i \leq c}$ . The input  $\mathcal{X}$  is given as a fully-packed ciphertext  $ct$ , and  $pt.F_j$  denotes a plaintext polynomial of the corresponding kernels. The operation  $*$  indicates the multi-channel convolution. The operation  $*_s$  indicates the parallelized simple convolution of a single input channel with a kernel over encryption.

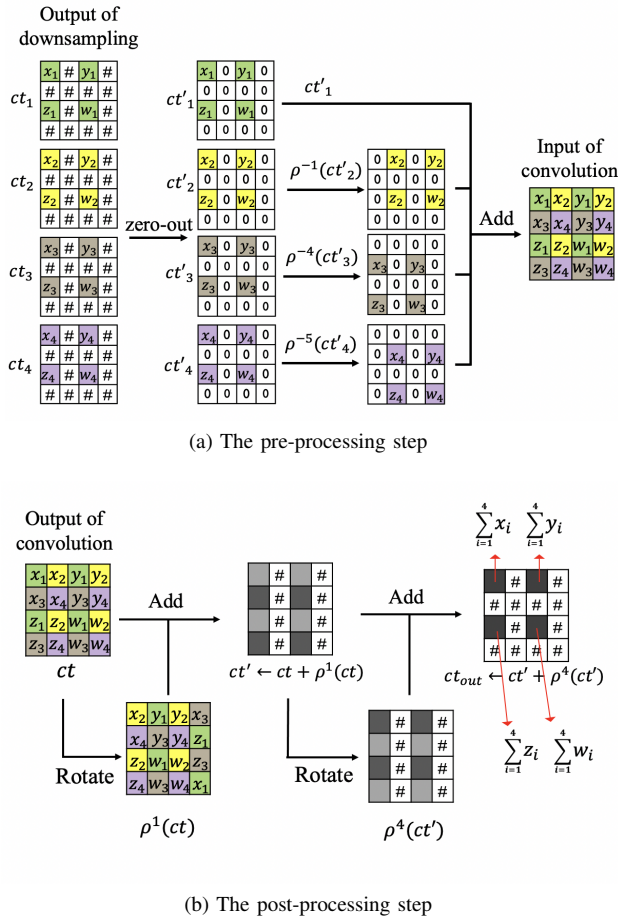


Fig. 5: The pre-processing and post-processing procedures for homomorphic convolution in Fast-HEAR. The colored entries are valid values as the output response maps of the pooling layer, whereas the junk entries marked # are non-valid values.

for  $1 \leq i \leq \sqrt{n_P} - 1$ ,  $0 \leq k < \sqrt{n_P}$ ,  $1 \leq j \leq \lceil \log_2(\sqrt{n_P}) \rceil$ , and  $k' = 0, 1$ .

#### D. Refinement of homomorphic convolution

The permutations on plaintext slots enable us to interact with values located in different plaintext slots; however, the

#### Algorithm 2 Fast homomorphic convolution

**Input:**  $\{ct_j\}_{1 \leq j \leq n_I}$   
**Output:**  $\{ct.res_j\}_{1 \leq j \leq n_O}$

**[Pre-processing step]**

- 1: **for**  $1 \leq j \leq n_I/n_P$  **do**
- 2:   **for**  $1 \leq i \leq n_P$  **do**
- 3:      $ct'_i \leftarrow \text{MultPlain}(ct_{i+(j-1) \cdot n_P}, pt_{zone})$    // zero-out
- 4:   **end for**
- 5:   **for**  $2 \leq i \leq n_P$  **do**
- 6:      $ct'_i \leftarrow \text{Add}(ct'_1, \text{Rot}(ct'_i, -\mu_i))$    // aggregation
- 7:   **end for**
- 8:    $ct.pre_j \leftarrow \text{Rescale}(ct.pre_j)$
- 9: **end for**

**[Homomorphic convolution]**

- 10: **for**  $1 \leq j \leq n_O$  **do**
- 11:    $ct.conv_j \leftarrow \text{H-Conv}_j(ct.pre_1, \dots, ct.pre_{n_I/n_P})$
- 12: **end for**

**[Post-processing step]:**

- 13: **for**  $1 \leq j \leq n_O$  **do**
- 14:    $ct.res_j \leftarrow ct.conv_j$
- 15:   **for**  $1 \leq i \leq \lceil \log_2(n_P) \rceil$  **do**
- 16:      $ct.res_j \leftarrow \text{Add}(ct.res_j, \text{Rot}(ct.res_j; \nu_i))$
- 17:   **end for**
- 18: **end for**
- 19: **return**  $\{ct.res_j\}_{1 \leq j \leq n_O}$

computational costs of these operations are relatively more expensive than addition and multiplication. So, we aim to reduce the number of automorphisms by applying the idea of the baby-step/giant-step algorithm [22]. We elaborate on the efficient implementation of Eq. (3) for homomorphic convolutions. (i) *Full-step* strategy: We pre-compute all the rotated ciphertexts of the form  $\rho^{r_k+h \cdot w \cdot \ell}(ct_i)$  and perform constant-ciphertext multiplications, which takes  $(f \cdot \ell_I - 1) \cdot n_I$  automorphisms. (ii) *Giant-step* strategy: Eq. (3) can be reformulated as

$$\sum_k \rho^{r_k} \left( \sum_{i, \ell} (\rho^{h \cdot w \cdot \ell}(ct_i) \cdot \rho^{-r_k}(pt.F_{i,j,k,\ell})) \right). \quad (4)$$

TABLE I: The computational cost of the convolutional layers in HEAR and Fast-HEAR. Rot denotes the ordinary rotation which cannot benefit from hoisting, and Hoisted Rot denotes multiple rotations on the same input ciphertext that can benefit from the hoisting optimization. H-Rot<sub>k</sub> requires  $(k - 1)$  rotations on an input ciphertext).

Method	Method	Homomorphic operations count			
		Rot	Hoisted Rot	MultPlain	Rescale
HEAR	Full-step	—	$n_I \cdot \text{H-Rot}_{f \cdot \ell_I}$	$f \cdot \ell_I \cdot \frac{n_I}{n_P} \cdot n_O$	$n_O$
	Giant-step	$(f - 1) \cdot n_O$	$n_I \cdot \text{H-Rot}_{\ell_I}$		
	Baby-step	$(\ell_I - 1) \cdot n_O$	$n_I \cdot \text{H-Rot}_f$		
Fast-HEAR	Full-step	$(n_P - 1) \cdot \frac{n_I}{n_P} + n_O \cdot \log_2 n_P$	$\frac{n_I}{n_P} \cdot \text{H-Rot}_{f \cdot \ell_I}$	$n_I + f \cdot \ell_I \cdot \frac{n_I}{n_P} \cdot n_O$	$n_O + \frac{n_I}{n_P}$
	Giant-step	$(n_P - 1) \cdot \frac{n_I}{n_P} + n_O \cdot \log_2 n_P + (f - 1) \cdot n_O$	$\frac{n_I}{n_P} \cdot \text{H-Rot}_{\ell_I}$		
	Baby-step	$(n_P - 1) \cdot \frac{n_I}{n_P} + n_O \cdot \log_2 n_P + (\ell_I - 1) \cdot n_O$	$\frac{n_I}{n_P} \cdot \text{H-Rot}_f$		

This method is to pre-compute the rotated giant ciphertexts  $\rho^{h \cdot w \cdot \ell}(\text{ct}_i)$ 's for  $i$  and  $\ell$ , sum up the products, and perform the evaluation of  $\rho^{r \cdot k}$ . So it needs  $(\ell_I - 1) \cdot n_I$  automorphisms for the giant-step and additional  $(f - 1) \cdot n_O$  automorphisms. (iii) *Baby-step* strategy: The equation can be expressed as

$$\sum_{\ell} \rho^{r \cdot \ell} \left( \sum_{i,k} (\rho^{r \cdot k}(\text{ct}_i) \cdot \rho^{-r \cdot \ell}(\text{pt} \cdot \text{F}_{i,j,k,\ell})) \right). \quad (5)$$

So, one can pre-compute the rotated baby ciphertexts  $\rho^{r \cdot k}(\text{ct}_i)$ 's for  $i$  and  $k$ , aggregate the products, and perform the evaluation of  $\rho^{r \cdot \ell}$ . It requires  $(f - 1) \cdot n_I$  automorphisms for the baby-step and additional  $(n_I - 1) \cdot n_O$  automorphisms.

Note that we can benefit from the *hoisting* optimization of [22] to reduce the complexity of multiple rotations on the same input ciphertext. We can compute only once the common part that involves the computation of the Number Theoretic Transformation (NTT) conversion on the input (of  $\Theta(N \log N)$  complexity). As a result, the required number of NTT conversions can be reduced from  $k$  to 1 if we use hoisting optimization on  $k$  rotations of a ciphertext instead of applying each one separately. In Table I, we provide the detailed computational costs of the convolutional layers in the HEAR and Fast-HEAR systems. The evaluation strategies show different performance tendencies on the number of input/output ciphertexts.

### E. Non-convolutional layers

1) *Low-degree polynomial activation*: We replace the ReLU activation with a quadratic polynomial and the coefficients are adjusted during the training phase. As shown in Table II, we observed that our network with degree-2 polynomial activation brings no accuracy loss compared to ReLU activation.

2) *Collapsing consecutive layers*: Previous studies [10], [20] collapsed adjacent linear layers such as convolution and pooling layers. On the other hand, we observe that the following layers can be collapsed while maintaining the same network structure: addition of a bias term in the convolution, BN, activation, and scaling operation of the average pooling. Since we adjust these parameters during the training phase, they can be pre-computed before private inference. As a result, the collapsed layers become degree-2 polynomial evaluation

TABLE II: Accuracy comparison of our degree-2 polynomial approximation and ReLU function for action recognition.

Method	Our approach	ReLU
1D-CNN	0.8701	0.8372
2D-CNN	0.8799	0.8782

per feature map, which will be applied to the elements of the same feature map in a SIMD manner.

To be precise, for each feature map, suppose that we are given the following parameters : (i) learned bias  $b$  of the convolution layer; (ii) BN statistics  $(\mu, \sigma, \gamma, \beta)$ ; (iii) coefficient parameters of an activation function  $(a_0, a_1, a_2)$  such that the activation is defined as  $x \mapsto a_0 + a_1 x + a_2 x^2$ ; (iv) window size  $(s_1, s_2)$  of the average pooling layer. We recall the BN of [26]. We denote by  $x$  an output value of a convolutional layer of the network without adding the bias term. Then it is updated as follows:

$$z = \gamma \left( \frac{(x + b) - \mu}{\sigma} \right) + \beta = d_0 + d_1 \cdot x, \quad (6)$$

where  $d_1 = \gamma/\sigma$  and  $d_0 = \beta + d_1(b - \mu)$ . Afterward, the output is activated as

$$a_0 + a_1 z + a_2 z^2 = (a_0 + a_1 \cdot d_0 + a_2 \cdot d_0^2) + (a_1 \cdot d_1 + 2 \cdot a_2 \cdot d_0 \cdot d_1)x + (a_2 \cdot d_1^2)x^2. \quad (7)$$

In the end, we sum up all the parameters and it suffices to evaluate the following function  $x \mapsto c_0 + c_1 \cdot x + c_2 \cdot x^2$  where

$$\begin{aligned} c_0 &= \frac{a_0 + a_1 \cdot d_0 + a_2 \cdot d_0^2}{s_1 \cdot s_2}, \\ c_1 &= \frac{a_1 \cdot d_1 + 2 \cdot a_2 \cdot d_0 \cdot d_1}{s_1 \cdot s_2}, \\ c_2 &= \frac{a_2 \cdot d_1^2}{s_1 \cdot s_2}. \end{aligned} \quad (8)$$

To be precise, we let  $c_{n,m}^t$  be the  $m$ -th coefficient of the  $n$ -th feature map at the  $t$ -th block of the network. For  $1 \leq j \leq n_O^t$ , we denote by  $\text{pt.coeff}_{j,m}^t$  a plaintext polynomial of the vector obtained by concatenating the  $m$ -th coefficients  $c_{n,m}^t$ 's for  $\ell_O^t \cdot (j - 1) < n \leq \ell_O^t \cdot j$ .

3) *Fully-connected layer*: After feature extraction, the final  $d_I$  outputs of the activation function feed a fully connected layer with  $d_O$  output neurons. Let  $W$  and  $v$  be the  $(d_O \times d_I)$  weight matrix and length- $d_I$  vector, respectively. Suppose that the output vector of the global average pooling layer  $v$  is given as multiple ciphertexts, each of which has  $c$  values of the input vector in a sparse way. We split  $v$  into sub-strings  $v_i$ 's with the same length  $c$ . Accordingly, we split the original matrix  $W$  into  $(d_O \times c)$ -sized smaller blocks  $W_i$  and perform computation on the sub-matrices:

$$W \cdot v = \sum_{1 \leq i \leq d_I/c} W_i \cdot v_i.$$

We apply the diagonal encoding method of the matrix-vector multiplication [21] to the computation on the sub-matrices: it puts a square matrix in a diagonal order, multiplies each of them with a rotation of the input vector, and then sums up all the output vectors to obtain the result. Consequently, the output ciphertext has  $d_O$  predicted results. To be specific, they can be obtained by taking the first  $d_O$  entries of the vector

$$\sum_{\substack{1 \leq i \leq d_I/c, \\ 1 \leq \ell \leq c}} \text{Diag}_\ell(\text{padZeros}(W_i; c - d_O, B)) \odot \rho^\ell(v_i), \quad (9)$$

where  $\text{Diag}_\ell(A)$  indicates the  $\ell$ -th diagonal component of a square matrix  $A$ . Note that the data vector  $v_i$  is given as the ciphertext  $\text{ct}_i$  that represents the entries in a sparsely-packed way. For the sake of brevity, let  $W_{i\ell} = \text{Diag}_\ell(\text{padZeros}(W_i; c - d_O, B))$ . So, Eq. (9) can be securely computed as follows:

$$\sum_{i,\ell} \text{Encode}(W_{i\ell}) \cdot \rho^{\text{dist} \cdot \ell}(\text{ct}_i), \quad (10)$$

where  $\text{dist}$  denotes the distance of two valid entries of  $v_i$  over plaintext slots (which is  $N_2/c = N_2/\ell_O^3 = \text{PoT}(T \cdot J)$ ). Then it requires  $(d_I/c) \cdot c = d_I$  rotations to compute Eq. (10). We reformulate this equation:

$$\sum_{\ell} \rho^{\text{dist} \cdot \ell} \left( \sum_i \text{pt} \cdot W_{i\ell} \cdot \text{ct}_i \right),$$

where  $\text{pt} \cdot W_{i\ell} = \text{Encode}(\rho^{-\text{dist} \cdot \ell}(W_{i\ell}))$ . Then it reduces the number of rotations down to  $c$ , achieving a performance gain.

#### IV. EXPERIMENTAL METHODOLOGY

We explain how to select HE parameters to achieve the desired security and enable efficient implementation. We empirically demonstrate the action recognition performance of the proposed method over benchmark datasets.

##### A. Encryption parameter selection

We employ the Residue Number System (RNS) variant of the CKKS scheme [12] to achieve an efficiency of homomorphic operations. We multiply a scale factor of  $\Delta$  to plaintexts and perform the rescaling procedure by a factor of  $\Delta$  on ciphertexts after each multiplication to maintain the precision of the plaintext, which means that a ciphertext modulus is reduced by  $\log_2 \Delta$  bits after multiplication or a

TABLE III: Homomorphic encryption parameters for HEAR and Fast-HEAR.  $q_0$  is the output ciphertext modulus.  $q_{\text{msg}}$  is the scaling factor for an input tensor and weight parameters (in HEAR,  $p_i$ 's for  $1 \leq i \leq 10$ ; in Fast-HEAR,  $p_i$ 's for  $1 \leq i \leq 12$  except  $i = 5, 9$ ).  $p_{\text{mask}}$  is the scaling factor for multiplicative masking vectors in Fast-HEAR (the RNS primes of  $p_5$  and  $p_9$ ). The special modulus  $p$  is chosen to reduce the noise growth during homomorphic operations.

Method	Parameters					
	$L$	$\log_2 q$	$\log_2 q_0$	$\log_2 p_{\text{msg}}$	$\log_2 p_{\text{mask}}$	$\log_2 p$
HEAR	10	387	37	35	-	37
Fast-HEAR	12	399	33	31	28	33

multiplication operation consumes one level. We set the scale factor  $\Delta_{\text{msg}} = 2^{31}$  or  $2^{33}$  for an input tensor and weight parameters in HEAR and Fast-HEAR systems. We use a smaller scale factor  $\Delta_{\text{mask}} = 2^{28}$  for multiplicative masking vectors in Fast-HEAR. It requires 10 levels to implement the network architecture of HEAR, whereas Fast-HEAR needs two additional levels of constant-ciphertext multiplications for the pre-processing step. A rigorous analysis of level consumption will be provided later. In particular,  $q_0$  is chosen to guarantee the accuracy of two bits before the decimal point. In particular, we take a special modulus  $p$  such that  $\log_2 p \approx 33$  or  $\log_2 p \approx 37$ . We use uniform ternary secret distribution (i.e., the uniform distribution over the set of polynomials whose coefficients are in  $\{-1, 0, 1\}$ ). Each coefficient of an error is drawn according to the discrete Gaussian distribution centered at zero with standard deviation  $\sigma = 3.2$ . In the end, we take the ciphertext ring dimension  $N = 2^{14}$  to ensure 128 bits of security against the known attacks on the LWE problem from the LWE estimator [3] and HE security standard white paper [2]. The encryption parameters are summarized in Table III.

##### B. Cryptographic optimizations

We adopt three optimizations of homomorphic computation.

- **Hoisting optimization**: One can compute the common part of multiple rotations on the same input ciphertext as noted in Section III-B. In Table IV, we present detailed benchmarks for the impact of the hoisting technique with various numbers of rotated ciphertexts.
- **Lazy-rescaling**: We do not have to perform rescaling after every multiplication. For instance, when evaluating Eq. (3), we can first compute products between plaintext polynomials and ciphertexts, sum up all the resulting ciphertexts, and perform the rescaling operation only once to adjust the scaling factor of the output ciphertext.
- **Level-aware model parameter encoding**: When using plaintext polynomials of the trained model parameters, only a small subset of polynomial coefficients is needed for computation. To be precise, for each plaintext, we can pre-determine the maximal level  $\ell$  of ciphertexts to be computed with the plaintext, and only  $(\ell + 1)$  RNS



TABLE IV: Hoisting benchmarks with the same HE parameters as Fast-HEAR on a single thread execution environment.

Number of rotated ciphertexts	Naive approach	Hoisting	Speedup
4	222.1 ms	126.7 ms	1.8×
16	899.9 ms	426.2 ms	2.1×
64	3544.7 ms	1596.7 ms	2.2×

primes are used to generate the plaintext. Consequently, we can reduce the encoding running time and memory usage from  $O(L)$  down to  $O(\ell)$ .

In the following, we will investigate how ciphertext levels change during homomorphic evaluation of our three-layered network models and deduce the optimized encoding levels of weight parameters. We start with the network input ciphertext  $ct_{\mathcal{X}}$  at level  $L$  in the HEAR system. Each convolutional layer of the network has a depth of one constant-ciphertext multiplication, and the collapsed layer of BN and activation requires a depth of one constant-ciphertext multiplication and ciphertext-ciphertext multiplication. Finally, the fully-connected layer has a depth of one constant-ciphertext multiplication. Let  $pt.F_t$  be the plaintext polynomials of the kernels at the  $t$ -th convolutional layer. Let  $pt.coeff_t^k$  be the plaintext polynomials of the coefficient of degree- $k$  approximation of the  $t$ -th activation. Let  $pt.W$  be the plaintext polynomials of the weight matrix at the fully-connected layer. We then get the following minimum encoding levels of the model parameters:

- $level(pt.F_t) = L - 3 \cdot (t - 1)$ ,
- $level(pt.coeff_t^k) = \begin{cases} level(pt.F_t) - 3, & \text{if } k = 0; \\ level(pt.F_t) - 2, & \text{otherwise,} \end{cases}$
- $level(pt.W) = level(pt.F_3) - 3$ ,

It suffices to satisfy the inequality  $1 \leq level(pt.W) = (L - 3 \cdot (3 - 1)) - 3$ . Therefore, we deduce that the level of the input ciphertext  $L$  is set to 10.

In the context of the Fast-HEAR system, the encoding levels for the kernels are  $level(pt.F_t) = L - 4 \cdot (t - 1)$  as we need constant zero-one vectors to remove junk entries right after pooling layers. So, the encoding levels for the first and second pooling layers are  $level(pt.F_t) - 3$  for  $t = 1, 2$ . As a result, the level of the input ciphertext  $L$  is set to 12.

## V. EXPERIMENTAL RESULTS

### A. Experiment setup

1) *Dataset*: Our dataset contains two categories of data: (1) Activities of Daily Living (ADL) was selected from the J-HMDB dataset [27]. The selected action classes are clap, jump, pick, pour, run, sit, stand, walk, and wave, resulting in 376 videos in total. (2) The dataset for fall action class was created by merging the UR Fall Detection dataset (URFD) [33] and the Multiple cameras fall dataset (Multicam) [6]. URFD contains 30 fall videos and Multicam contains 22 fall videos from 8 different perspectives. The datasets are randomly split

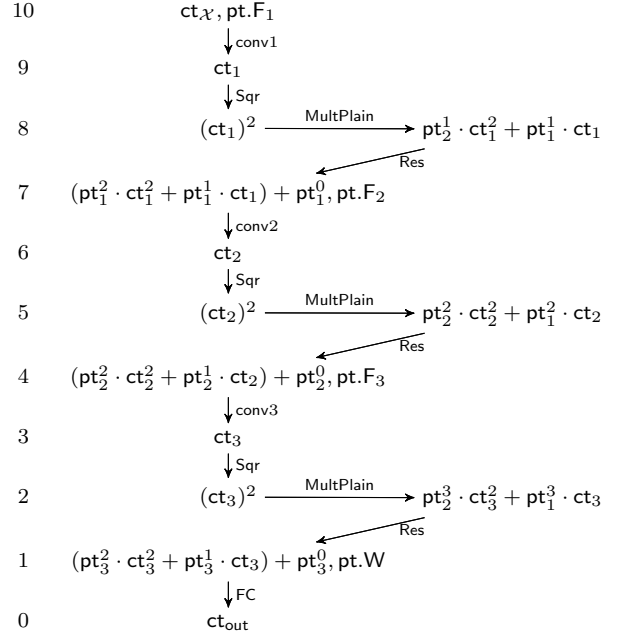


Fig. 6: An illustration of the evaluation procedure of HEAR. For the sake of brevity, we let  $pt_t^k = pt.coeff_t^k$ .

into training, validation, and testing sets containing 70% (84 falls and 264 no-falls), 10% (10 falls and 36 no-falls), and 20% (29 falls and 75 no-falls), respectively.

2) *Data pre-processing*: Following recent studies [38], [49], [51] to simplify the action recognition task and eliminate background noise, we transform the skeleton joints into a pseudo-image while preserving their spatial-temporal information, which is fed into a CNN model to extract the feature and classify the action.

The network for human pose estimation utilizes the Deep High-Resolution network [45] pre-trained with the MPII Human Pose dataset [5]. So, the output of the network is locations of ankles, knee, hip, shoulder, wrist elbow, upper neck, and head top, providing 15 joint locations. Each joint location is encoded to a 2D coordinate  $(x, y)$ . The coordinate value for the undetected joints or detected ones with low probability is set as zero.

For the frame selection mechanism, we calculate the Euclidean distance for the corresponding joints location for two consecutive frames. We calculate the mean of the distances to calculate the interchangeability score for the frames. If the score is below the pre-defined threshold 5, the frame is dropped until we reach the required number of the selected frames. This mechanism ensures that the action recognition network is independent of the Frame per second (FPS) rate of the video camera.

The joint location values are normalized separately for the  $x$  and  $y$  coordinates in a way that the maximum and minimum of  $x$  and  $y$  for all predicted joints in each frame are calculated

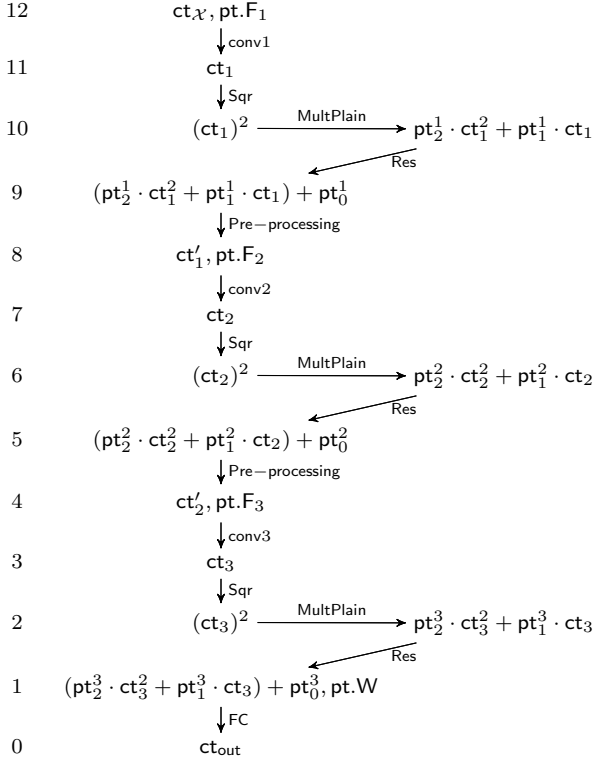


Fig. 7: An illustration of the evaluation procedure of Fast-HEAR.

and the coordinates are normalized as follows:

$$x \leftarrow \frac{x - \min x}{\max x - \min x}, \quad y \leftarrow \frac{y - \min y}{\max y - \min y}.$$

The normalization ensures that the action recognition network can work independently of the size of the body or the distance to the camera. Afterward, the  $x$  and  $y$  coordinates of all joint coordinates in each frame are separately concatenated in a way that the spatial structure of each frame is represented as rows and the temporal dynamics across the frames in a video is encoded as changes in columns, resulting in a 3D tensor of size  $32 \times 15 \times 2$  (i.e.,  $T = 32$  is the number of frames in the video).

3) *Network architecture*: We used Stochastic Gradient Decent (SGD) optimizer with a mini-batch size of 64, a momentum of 0.9, and a weight decay of  $5e^{-4}$  to train the model for 200 epochs. The initial learning rate was set to 0.05 with a decay of 0.1. In our experiments, we use a stack of three layers with 1D or 2D convolutions and study one small net and one large net: CNN-W64 and CNN-W128, where 64 and 128 represent the widths of the first convolutional layer, respectively. Table V summarizes the network architecture.

4) *Evaluation setup*: Our experiments were conducted on a machine with Intel Xeon Platinum 8268 2.9GHz CPU with a 16-thread environment using the ‘-O2’ optimization setting. Our source code is developed by modifying Microsoft SEAL version 3.4 [41].

TABLE V: The network architecture of our action recognition network. conv $i$  indicates the  $i$ -th convolutional layer.

Method		Layers		
		conv1	conv2	conv3
1D-CNN-W64	Output map size	480	240	120
	# Filters	64	128	256
1D-CNN-W128	Output map size	480	240	120
	# Filters	128	256	512
2D-CNN-W64	Output map size	(32, 15)	(16, 7)	(8, 3)
	# Filters	64	128	256
2D-CNN-W128	Output map size	(32, 15)	(16, 7)	(8, 3)
	# Filters	128	256	512

### B. Benchmark for homomorphic convolution

Table VI summarizes the number of input ciphertexts  $n_I$ , the number of output ciphertexts  $n_O$ , and the number of input ciphertexts  $n_P$  to fit into a single ciphertext for fast homomorphic convolution operation in the Fast-HEAR system. The column for HEAR gives timing for homomorphic convolution. The three columns for Fast-HEAR correspond to pre-processing step, ordinary homomorphic convolution, and post-processing step. The total running time of these procedures is given in the following column. The last column gives the speedup of homomorphic convolution in Fast-HEAR compared to HEAR.

At 1D-CNN, we get the load factor  $n_P^t$  as follows:

$$n_P^t = \begin{cases} \min\{n_I^t, 2\}, & \text{if } t = 2; \\ \min\{n_I^t, 4\}, & \text{if } t = 3. \end{cases}$$

On the other hand, at 2D-CNN, we get the number of  $n_P^t$  as follows:

$$n_P^t = \begin{cases} \min\{n_I^t, 2^2\}, & \text{if } t = 2; \\ \min\{n_I^t, 4^2\}, & \text{if } t = 3. \end{cases}$$

As discussed in Section III-C, we get a speedup of up to  $n_P$  for ordinary homomorphic convolution operation in Fast-HEAR compared to HEAR. So, we may offer more performance benefit as many as ciphertexts we can assemble. For example, the third convolutional layer in the 2D-CNN-W128 network has a load factor of  $n_P = 16$ , achieving a significant performance gain over HEAR. On the other hand, it requires additional costs for pre/post-processing procedures, resulting in a smaller speedup for the whole convolutional layer in practice.

### C. Results of homomorphic encrypted action recognition

An encrypted input tensor of the network has approximately 1.6 MB and it takes 40 milliseconds (ms) to encrypt one single input. After the evaluation, the cloud server outputs a single ciphertext of the predicted results, and it takes around 1.7 ms for decryption. In Table VII, we report timing results for the evaluation of HEAR and Fast-HEAR. It takes 12.2 seconds and 3.1 seconds on HEAR and Fast-HEAR to perform a single prediction on the 2D-CNN-W128 network, respectively. The intensive use of SIMD computation in Fast-HEAR offers a

TABLE VI: Benchmark of homomorphic convolution in our action recognition network.  $\text{conv}_i$  denotes the  $i$ -th convolutional layer in the network.

Method	Layer	# Ciphertexts			HEAR Conv	Timing (ms)				Speedup
		Input $n_I$	Output $n_O$	Packed $n_P$		Pre-pro.	Fast-HEAR Conv	Post-pro.	Total	
1D-CNN-W64	conv2	4	8	2	555.7	80.1	337.3	53.1	470.5	1.2×
	conv3	8	16	4	631.1	52.3	189.9	36.7	278.9	2.3×
1D-CNN-W128	conv2	8	16	2	1158.2	78.7	899.1	54.5	1032.3	1.1×
	conv3	16	32	4	3377.2	50.2	642.9	57.1	750.2	4.5×
2D-CNN-W64	conv2	4	8	4	1089.2	100.7	582.7	88.3	771.7	1.4×
	conv3	8	16	8	1615.9	50.0	306.2	55.5	411.7	3.9×
2D-CNN-W128	conv2	8	16	4	<b>4868.5</b>	77.8	1268.5	89.8	<b>1436.1</b>	3.4×
	conv3	16	32	16	<b>6348.7</b>	57.4	385.1	112.0	<b>554.6</b>	11.5×

TABLE VII: Experimental results of action recognition.

Method	Performance metrics			Latency	
	Accuracy	Sensitivity	Specificity	HEAR	F-HEAR
1D-CNN-W64	0.8668	0.8621	0.9914	1.894 sec	<b>1.443 sec</b>
1D-CNN-W128	0.8701	0.8621	0.9914	5.150 sec	<b>2.758 sec</b>
2D-CNN-W64	0.8799	0.8621	0.9914	3.451 sec	<b>2.160 sec</b>
2D-CNN-W128	0.8799	0.8621	0.9914	12.203 sec	<b>3.091 sec</b>

significant performance advantage, so we get a speedup of up to 4 times. Since 2D-CNN uses a larger load factor of  $n_P$  than 1D-CNN, Fast-HEAR can achieve a substantial performance improvement over HEAR.

Our selection of parameter sets offers a trade-off between evaluation performance and output precision. The parameter in HEAR guarantees at least 9 bits of precision after the decimal point, that is, the infinity norm distance between encrypted evaluation and un-encrypted computation is bounded by  $2^{-9}$ . Meanwhile, the parameter in Fast-HEAR guarantees at least 5 bits of precision after the decimal point. In our experiments, 5 bits of precision on the outputs of the network were sufficient in guaranteeing the accuracy of the neural network. As a result, our secure inference solution achieves the same accuracy of 86.68%~87.99% on the test set as the one obtained from the evaluation on the plaintext dataset. The algorithms are also evaluated in terms of typical performance metrics such as sensitivity or specificity, which are estimated from a ratio depending on the number of false and true positives and negatives that are achieved. The sensitivity and specificity of our model for fall detection are 86.21% and 99.14%, respectively.

#### D. Ablation study

We empirically analyze the effect of state-of-the-art techniques in our approach. (i) W/o lazy rescaling, (ii) W/o hoisting, (iii) W/ both lazy rescaling and hoisting techniques (this is our proposed method). The results on Fast-HEAR given in Table VIII show that the lazy rescaling optimization results in a substantial performance improvement because the naive method performs rescaling operations as many as constant-ciphertext multiplications that retain a significant portion of the whole process. The hoisting optimization does

TABLE VIII: Ablation study of cryptographic optimizations in the 2D-CNN-W128 of Fast-HEAR.

Method	Hoisting	Lazy rescaling	Latency	Speedup
F	✓		9.748 sec	1.02×
	✓	✓	3.567 sec	2.78×
G	✓		3.091 sec	3.21×
	✓	✓	9.606 sec	1.01×
B	✓		3.375 sec	2.87×
	✓	✓	3.357 sec	2.89×
	✓		10.030 sec	0.99×
	✓	✓	3.670 sec	2.73×
			3.661 sec	2.74×

not indicate significant improvement as much as in the lazy rescaling optimization. Nevertheless, the full-step strategy with optimization leads to the best performance because more ciphertexts can benefit from hoisting optimization. We refer to the supplementary material for additional experimental results of different baby-step/giant-step strategies with various numbers of threads.

As described in Section IV-B, the adjusted level-aware encoding brings about several benefits – reduce encoding time and memory usage. Table IX shows that the encoding time and memory usage of the trained model parameters can be reduced to half in both HEAR and Fast-HEAR systems when the adjusted level-aware encoding technique is used with information on ciphertext levels as in Section IV-B. As mentioned in Section III-C, the Fast-HEAR system reduces the number of plaintexts by a factor of  $n_P$  while using less space and time for model encoding. This results in a significant reduction in performance when using a larger load factor  $n_P$ . For example, when the 2D-CNN-W128 network is evaluated, we use the parameters  $n_P^2 = 4$  and  $n_P^3 = 16$  at the second and third convolutional layers, so Fast-HEAR is roughly 7 times faster than HEAR to encode the weight parameters (2.9 sec vs 21.1 sec) while using 86% less space than HEAR implementation (8.3 GB vs 63.5 GB).

## VI. COMPARISON WITH PRIOR WORK

Table X compares Fast-HEAR against the state-of-the-art privacy-preserving neural network frameworks such as CryptoNets [20], LoLa [10], and CHET [17]. These frameworks were implemented with different HE schemes in different

TABLE IX: Ablation study of the adjusted level-aware encoding method.

Method	HEAR				Fast-HEAR			
	W/ level encoding		W/o level encoding		W/ level encoding		W/o level encoding	
	Timing	Storage	Timing	Storage	Timing	Storage	Timing	Storage
1D-CNN-W64	2.081 sec	5.399 GB	3.535 sec	10.789 GB	0.999 sec	1.944 GB	1.633 sec	4.222 GB
1D-CNN-W128	7.558 sec	21.302 GB	12.206 sec	42.206 GB	2.583 sec	7.452 GB	4.618 sec	15.757 GB
2D-CNN-W64	5.651 sec	15.975 GB	9.556 sec	31.490 GB	1.525 sec	2.915 GB	2.566 sec	6.137 GB
2D-CNN-W128	<b>21.104 sec</b>	<b>63.458 GB</b>	37.196 sec	128.869 GB	<b>2.869 sec</b>	<b>8.379 GB</b>	5.121 sec	15.949 GB

TABLE X: Comparison with prior privacy-preserving neural network frameworks on our action recognition network 2D-CNN-W128.

Method	#Ciphertexts		HOC				
	Input	Output	Rot	Mult	MultPlain	Res	Total
CryptoNets	960	10	-	100K	62M	-	62M
LoLa	72	10	561K	6	41K	-	602K
CHET	1	1	4.4K	56	94K	1.2K	100K
<b>Fast-HEAR</b>	<b>1</b>	<b>1</b>	850	56	10K	172	<b>11K</b>

environments. For a fair comparison, we report the number of the required homomorphic operations for the evaluation of our action recognition network on the same dataset, which is independent of hardware configuration and software parallelization.

CryptoNets encrypts each node in the network individually and performs neural network inferencing computation in the normal way. So, the number of homomorphic operations is the same as the unencrypted neural network inferencing. On the other hand, both LoLa and CHET reduce the computational complexity by the ciphertext packing technique. In LoLa, the first convolution layer is represented as a restricted linear operation by flattening the filters to a single dimension. The subsequent convolutions are expressed as the product of a large weight matrix and an encrypted data vector. As a result, these simplifications bring a substantial number of rotation operations for an implementation of dot-product operations (as many as the size of output channels). Since we use wide networks with a considerably large number of channels, their solution is not perfectly optimized to our network. Compared to LoLa, Fast-HEAR reduces the number of rotation operations by 84.9% by the elaborated homomorphic convolutions. Similar to ours, although CHET represents an input tensor as a vector in row-major format, this system does not extensively use the plaintext space but simply pads zeros to the input. On the contrary, we replicate the data within the parameter limit, enabling more computation to be executed in parallel (with our optimized homomorphic convolutions) and resulting in a 9x speedup compared to CHET.

## VII. CONCLUSION

Homomorphic encryption has recently attracted much attention in the application of privacy-preserving *Machine Learning as a Service*. In this paper, we address the real-world challenge in privacy-preserving human action recognition by presenting

a scalable and low-latency HE-based system for secure neural network inference. To the best of our knowledge, this is the first secure model that can make predictions on daily activities and fall events. Our solution shows highly promising results for enhancing privacy-preserving real-time healthcare monitoring services for aging in place in a cost-effective and reliable manner.

## REFERENCES

- [1] “Aging in place,” <https://www.nia.nih.gov/health/topics/aging-place>, national Institute on Aging.
- [2] M. Albrecht, M. Chase, H. Chen, J. Ding, S. Goldwasser, S. Gorbunov, S. Halevi, J. Hoffstein, K. Laine, K. Lauter, S. Lokam, D. Micciancio, D. Moody, T. Morrison, A. Sahai, and V. Vaikuntanathan, “Homomorphic encryption security standard,” HomomorphicEncryption.org, Toronto, Canada, Tech. Rep., November 2018.
- [3] M. R. Albrecht, R. Player, and S. Scott, “On the concrete hardness of learning with errors,” *Journal of Mathematical Cryptology*, vol. 9, no. 3, pp. 169–203, 2015.
- [4] M. Alwan, S. Dalal, D. Mack, S. Kell, B. Turner, J. Leachtenauer, and R. Felder, “Impact of monitoring technology in assisted living: outcome pilot,” *IEEE Transactions on Information Technology in Biomedicine*, vol. 10, no. 1, pp. 192–198, 2006.
- [5] M. Andriluka, L. Pishchulin, P. Gehler, and B. Schiele, “2d human pose estimation: New benchmark and state of the art analysis,” in *Proceedings of the IEEE Conference on computer Vision and Pattern Recognition*, 2014, pp. 3686–3693.
- [6] E. Auvinet, C. Rougier, J. Meunier, A. St-Arnaud, and J. Rousseau, “Multiple cameras fall dataset,” *DIRO-Université de Montréal, Tech. Rep.*, vol. 1350, 2010.
- [7] M. Barni, C. Orlandi, and A. Piva, “A privacy-preserving protocol for neural-network-based computation,” in *Proceedings of the 8th workshop on Multimedia and security*, 2006, pp. 146–151.
- [8] F. Boemer, A. Costache, R. Cammarota, and C. Wierzynski, “ngraph-he2: A high-throughput framework for neural network inference on encrypted data,” in *Proceedings of the 7th ACM Workshop on Encrypted Computing & Applied Homomorphic Cryptography*, 2019, pp. 45–56.
- [9] F. Bourse, M. Minelli, M. Minihold, and P. Paillier, “Fast homomorphic evaluation of deep discretized neural networks,” in *Annual International Cryptology Conference*. Springer, 2018, pp. 483–512.
- [10] A. Brutzkus, R. Gilad-Bachrach, and O. Elisha, “Low latency privacy preserving inference,” in *Proceedings of the 36th International Conference on International Conference on Machine Learning*, 2019, pp. 812–821.
- [11] Z. Cao, T. Simon, S.-E. Wei, and Y. Sheikh, “Realtime multi-person 2d pose estimation using part affinity fields,” in *Proceedings of the IEEE conference on computer vision and pattern recognition*, 2017, pp. 7291–7299.
- [12] J. H. Cheon, K. Han, A. Kim, M. Kim, and Y. Song, “A full RNS variant of approximate homomorphic encryption,” in *Selected Areas in Cryptography – SAC 2018*. Springer, 2018, pp. 347–368.
- [13] J. H. Cheon, A. Kim, M. Kim, and Y. Song, “Homomorphic encryption for arithmetic of approximate numbers,” in *Advances in Cryptology–ASIACRYPT 2017: 23rd International Conference on the Theory and Application of Cryptology and Information Security*. Springer, 2017, pp. 409–437.

- [14] I. Chillotti, N. Gama, M. Georgieva, and M. Izabachène, “Faster fully homomorphic encryption: Bootstrapping in less than 0.1 seconds,” in *Advances in Cryptology—ASIACRYPT 2016: 22nd International Conference on the Theory and Application of Cryptology and Information Security*. Springer, 2016, pp. 3–33.
- [15] E. Chou, J. Beal, D. Levy, S. Yeung, A. Haque, and L. Fei-Fei, “Faster cryptonets: Leveraging sparsity for real-world encrypted inference. corr abs/1811.09953 (2018),” 2018.
- [16] R. Dathathri, B. Kostova, O. Saarikivi, W. Dai, K. Laine, and M. Musuvathi, “Eva: An encrypted vector arithmetic language and compiler for efficient homomorphic computation,” in *Proceedings of the 41st ACM SIGPLAN Conference on Programming Language Design and Implementation*, 2020, pp. 546–561.
- [17] R. Dathathri, O. Saarikivi, H. Chen, K. Laine, K. Lauter, S. Maleki, M. Musuvathi, and T. Mytkowicz, “CHET: an optimizing compiler for fully-homomorphic neural-network inferencing,” in *Proceedings of the 40th ACM SIGPLAN Conference on Programming Language Design and Implementation*, 2019, pp. 142–156.
- [18] Y. Du, Y. Fu, and L. Wang, “Skeleton based action recognition with convolutional neural network,” in *2015 3rd IAPR Asian Conference on Pattern Recognition (ACPR)*. IEEE, 2015, pp. 579–583.
- [19] Y. Du, W. Wang, and L. Wang, “Hierarchical recurrent neural network for skeleton based action recognition,” in *Proceedings of the IEEE conference on computer vision and pattern recognition*, 2015, pp. 1110–1118.
- [20] R. Gilad-Bachrach, N. Dowlin, K. Laine, K. Lauter, M. Naehrig, and J. Wernsing, “Cryptonets: Applying neural networks to encrypted data with high throughput and accuracy,” in *International Conference on Machine Learning*, 2016, pp. 201–210.
- [21] S. Halevi and V. Shoup, “Algorithms in HELib,” in *Advances in Cryptology—CRYPTO 2014*. Springer, 2014, pp. 554–571.
- [22] —, “Faster homomorphic linear transformations in HELib,” in *Annual International Cryptology Conference*. Springer, 2018, pp. 93–120.
- [23] K. He, G. Gkioxari, P. Dollár, and R. Girshick, “Mask r-cnn,” in *Proceedings of the IEEE international conference on computer vision*, 2017, pp. 2961–2969.
- [24] K. He, X. Zhang, S. Ren, and J. Sun, “Deep residual learning for image recognition,” in *Proceedings of the IEEE conference on computer vision and pattern recognition*, 2016, pp. 770–778.
- [25] M. E. Hussein, M. Torki, M. A. Gowayyed, and M. El-Saban, “Human action recognition using a temporal hierarchy of covariance descriptors on 3d joint locations,” in *Twenty-Third International Joint Conference on Artificial Intelligence*, 2013.
- [26] S. Ioffe and C. Szegedy, “Batch normalization: Accelerating deep network training by reducing internal covariate shift,” in *International Conference on Machine Learning*, 2015, pp. 448–456.
- [27] H. Jhuang, J. Gall, S. Zuffi, C. Schmid, and M. J. Black, “Towards understanding action recognition,” in *International Conf. on Computer Vision (ICCV)*, Dec. 2013, pp. 3192–3199.
- [28] C. Juvekar, V. Vaikuntanathan, and A. Chandrakasan, “GAZELLE: A low latency framework for secure neural network inference,” in *27th USENIX Security Symposium (USENIX Security 18)*, 2018, pp. 1651–1669.
- [29] Q. Ke, M. Bennamoun, S. An, F. Sohel, and F. Boussaid, “A new representation of skeleton sequences for 3d action recognition,” in *Proceedings of the IEEE conference on computer vision and pattern recognition*, 2017, pp. 3288–3297.
- [30] A. Kim, Y. Song, M. Kim, K. Lee, and J. H. Cheon, “Logistic regression model training based on the approximate homomorphic encryption,” *BMC Medical Genomics*, vol. 11, no. 4, p. 83, 2018.
- [31] M. Kim, Y. Song, S. Wang, Y. Xia, and X. Jiang, “Secure logistic regression based on homomorphic encryption: design and evaluation,” *JMIR medical informatics*, vol. 6, no. 2, 2018.
- [32] T. S. Kim and A. Reiter, “Interpretable 3d human action analysis with temporal convolutional networks,” in *2017 IEEE conference on computer vision and pattern recognition workshops (CVPRW)*. IEEE, 2017, pp. 1623–1631.
- [33] B. Kwolek and M. Kepski, “Human fall detection on embedded platform using depth maps and wireless accelerometer,” *Computer methods and programs in biomedicine*, vol. 117, no. 3, pp. 489–501, 2014.
- [34] E. H. Lee, D. Miyashita, E. Chai, B. Murmann, and S. S. Wong, “Lognet: Energy-efficient neural networks using logarithmic computation,” in *2017 IEEE International Conference on Acoustics, Speech and Signal Processing (ICASSP)*. IEEE, 2017, pp. 5900–5904.
- [35] J. Liu, M. Juuti, Y. Lu, and N. Asokan, “Oblivious neural network predictions via minionn transformations,” in *Proceedings of the 2017 ACM SIGSAC Conference on Computer and Communications Security*, 2017, pp. 619–631.
- [36] J. Liu, A. Shahroury, D. Xu, and G. Wang, “Spatio-temporal lstm with trust gates for 3d human action recognition,” in *European conference on computer vision*. Springer, 2016, pp. 816–833.
- [37] Q. Lou and L. Jiang, “SHE: A fast and accurate deep neural network for encrypted data,” in *Advances in Neural Information Processing Systems*, 2019, pp. 10035–10043.
- [38] D. Ludl, T. Gulde, and C. Curio, “Simple yet efficient real-time pose-based action recognition,” in *2019 IEEE Intelligent Transportation Systems Conference (ITSC)*. IEEE, 2019, pp. 581–588.
- [39] C. Orlandi, A. Piva, and M. Barni, “Oblivious neural network computing via homomorphic encryption,” *EURASIP Journal on Information Security*, vol. 2007, pp. 1–11, 2007.
- [40] C. N. Scanail, S. Carew, P. Barralon, N. Noury, D. Lyons, and G. M. Lyons, “A review of approaches to mobility telemonitoring of the elderly in their living environment,” *Annals of biomedical engineering*, vol. 34, no. 4, pp. 547–563, 2006.
- [41] “Microsoft SEAL (release 3.4),” <https://github.com/Microsoft/SEAL>, Oct. 2019, microsoft Research, Redmond, WA.
- [42] A. Shahroury, J. Liu, T.-T. Ng, and G. Wang, “Ntu rgb+ d: A large scale dataset for 3d human activity analysis,” in *Proceedings of the IEEE conference on computer vision and pattern recognition*, 2016, pp. 1010–1019.
- [43] C. Si, Y. Jing, W. Wang, L. Wang, and T. Tan, “Skeleton-based action recognition with spatial reasoning and temporal stack learning,” in *Proceedings of the European Conference on Computer Vision (ECCV)*, 2018, pp. 103–118.
- [44] S. Song, C. Lan, J. Xing, W. Zeng, and J. Liu, “An end-to-end spatio-temporal attention model for human action recognition from skeleton data,” in *Thirty-first AAAI conference on artificial intelligence*, 2017.
- [45] K. Sun, B. Xiao, D. Liu, and J. Wang, “Deep high-resolution representation learning for human pose estimation,” in *Proceedings of the IEEE Conference on Computer Vision and Pattern Recognition*, 2019, pp. 5693–5703.
- [46] R. Vemulapalli, F. Arrate, and R. Chellappa, “Human action recognition by representing 3d skeletons as points in a lie group,” in *Proceedings of the IEEE conference on computer vision and pattern recognition*, 2014, pp. 588–595.
- [47] J. Wang, Z. Liu, Y. Wu, and J. Yuan, “Mining actionlet ensemble for action recognition with depth cameras,” in *2012 IEEE Conference on Computer Vision and Pattern Recognition*. IEEE, 2012, pp. 1290–1297.
- [48] S. Yan, Y. Xiong, and D. Lin, “Spatial temporal graph convolutional networks for skeleton-based action recognition,” in *Thirty-second AAAI conference on artificial intelligence*, 2018.
- [49] F. Yang, Y. Wu, S. Sakti, and S. Nakamura, “Make skeleton-based action recognition model smaller, faster and better,” in *Proceedings of the ACM Multimedia Asia*, 2019, pp. 1–6.
- [50] P. Zhang, C. Lan, J. Xing, W. Zeng, J. Xue, and N. Zheng, “View adaptive recurrent neural networks for high performance human action recognition from skeleton data,” in *Proceedings of the IEEE International Conference on Computer Vision*, 2017, pp. 2117–2126.
- [51] M. Zolfaghari, G. L. Oliveira, N. Sedaghat, and T. Brox, “Chained multi-stream networks exploiting pose, motion, and appearance for action classification and detection,” in *Proceedings of the IEEE International Conference on Computer Vision*, 2017, pp. 2904–2913.

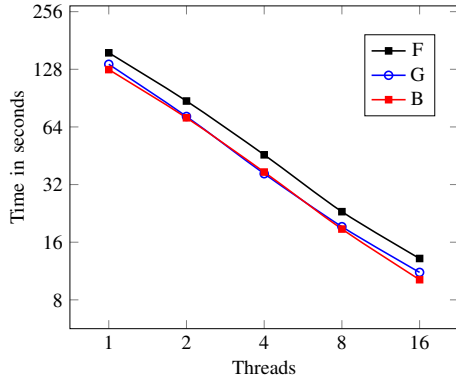
## APPENDIX

### A. EXPERIMENTAL RESULTS

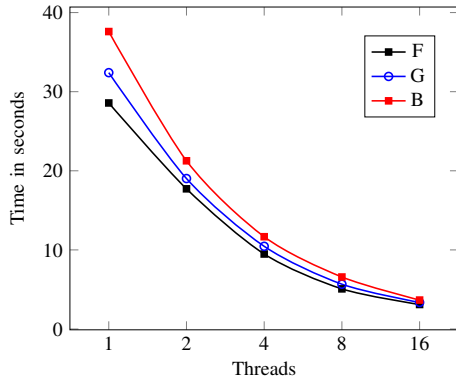
Fig. 8 shows the timing results of different homomorphic convolution methods with respect to various number of available threads. Our implementation exploits multiple cores, when available, and these results show that at least up to 16 cores the speedups scale linearly with the number of cores in all the methods.

The confusion matrix for our system is shown in Fig. 9.



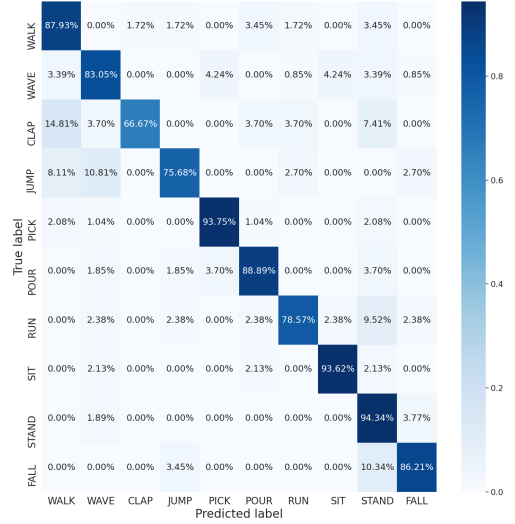


(a) Experimental result of HEAR.

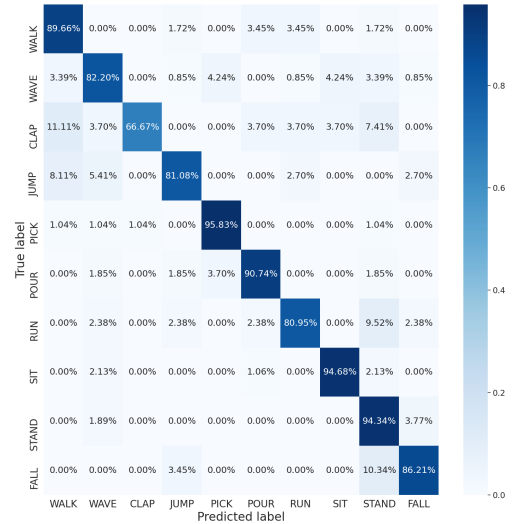


(b) Experimental result of Fast-HEAR.

Fig. 8: Average latency with respect to various threads (log-log scale).



(a) 1D-CNN



(b) 2D-CNN

Fig. 9: The confusion matrix of the action network on the validation set.